Nuclear Physics A473 (1987) 365-393
North-Holland, Amsterdam

NUCLEAR MEAN FIELD WITH CORRELATIONS AT FINITE TEMPERATURE*

P. GRANGE

Centre de Recherches Nucléaires, B.P. 20 CRO, F-67037 Strasbourg Cedex, France

J. CUGNON and A. LEJEUNE

Université de Liège, Physique Nucléaire Théorique, Institut de Physique au Sart Tilman, B.5, B-4000 Liège 1, Belgique

Received 4 March 1987
(Revised 25 May 1987)

Abstract: Zero and finite temperature contributions of ground state correlations to the nuclear mean field are studied in nuclear matter at normal density. The framework is the nonrelativistic hole line expansion with the Paris potential as the bare NN interaction. For different temperatures we calculate single particle properties including correlation contributions in the self-consistent determination of the single-particle energies. We evaluate the nucleon effective mass and the energy mass. Their temperature dependence is studied and related to that of the level density parameter. We also calculate the momentum distribution of nucleons and discuss its behaviour at large momenta. In the present approach the spectral function and the lifetime of hole state can be obtained directly. We present our first results and analyze them briefly. Finally, we examine the important aspects of the conserving character of the approximations made in the course of this study.

1. Introduction

The knowledge of the single-particle properties is of basic importance in nuclear physics for the understanding of nuclear structure and nuclear dynamics. Quantities like the mean field, the nucleon mean free path, the effective mass, enter in the description of static as well as dynamic properties of nuclei. Important progress has been accomplished during the past ten years in the calculation of single-particle quantities from first principles, after the work of ref. [1]), based on nonrelativistic Brueckner theory. Recently, another important step has been made with the calculation of these quantities in the frame of a relativistic many-body theory [2]) of nuclear matter, constructed in the spirit of Brueckner theory. Despite the widely different mechanisms leading to the building up of the nuclear mean field in the two theories, the depth of this mean field surprisingly comes up with the same value in the two approaches, when both are limited to the first order in Brueckner renormalized interaction (the g-matrix). Other properties, like the energy or momentum dependence of the mean field are also qualitatively similar in the two approaches.

* Work supported by the NATO research grant no. 025.81.

Here, we want to go one step further and calculate the mean field inside nuclear matter, up to second order in the nonrelativistic g-matrix (a relativistic calculation is probably not feasible for the time being), at zero and finite temperature, so extending our recent work [3]). In particular we want to calculate the so-called correlation graph contribution to the nucleon self-energy, for a realistic interaction. We study the energy and temperature dependence of the optical-model potential, calculated at this level of approximation. Furthermore, we pay particular attention to the temperature dependence of the effective mass, a feature which could play an important role in the dynamics of nuclear excitations and in heavy ion reactions. We also discuss the level density parameter, the momentum distribution, the lifetime of hole states and other related quantities.

The present work is organized as follows. Sect. 2 is a reminder of Green's function formalism and establishes our notation. Sect. 3 is devoted to the correlation graph for the mass operator. We discuss successively the self-consistency requirement for the auxiliary potential and the evaluation of the real and imaginary parts of the optical-model potential. Sect. 4 is devoted to the nucleon effective mass and its temperature dependence, to the so-called E-mass and to the level density parameter. In sect. 5, we calculate the momentum distribution in nuclear matter. Sect. 6 is devoted to a short discussion of the spectral function and of the lifetime of hole states. In sect. 7, we present a discussion of the binding energy and of the Hugenholtz-Van Hove theorem always at the light of the second-order approximation. Finally, sect. 8 contains our conclusion.

2. The nucleon self-energy in nuclear matter

2.1. DEFINITION

The real time Green function $\bar{G}$ for a nucleon travelling inside uniform infinite symmetric nuclear matter at temperature $T=\beta^{-1}$ and at chemical potential μ, is defined, with the notation of ref. [4]), as

$$\bar{G}(r, t) = -i\langle \hat{T}\{\psi(r, t)\psi^{\dagger}(0, 0)\}\rangle , \tag{2.1}$$

where $\hat{T}$ is the chronological operator and where $\psi^{\dagger}$and ψ are the Heisenberg creation and destruction field operators. The brackets indicate the average over a grand canonical ensemble.

As is well known, the Green function (2.1) describes at the same time the propagation of a particle added and the propagation of a hole punched in the medium. The Fourier transformed Green function,*

$$\bar{G}(k, \omega) = \int \mathrm{d}^3 r \int \mathrm{d}t\, \mathrm{e}^{-i(k\cdot r-\omega t)}\bar{G}(r, t) , \tag{2.2}$$

* The invariance under translation removes the dependence upon the orientation of k.

can be written as the following integral (the Lehmann representation):

$$\bar{G}(k,\omega)=\int_{-\infty}^{+\infty}\frac{\mathrm{d}\omega'}{2\pi}S(k,\omega')\left\{\frac{\mathscr{P}}{\omega-\omega'}+i\pi\delta(\omega-\omega')\tanh\tfrac{1}{2}\beta\omega'\right\}, \tag{2.3}$$

where $\mathscr{P}$ denotes the principal value integral and where $S(k,\omega)$ is generally called the strength function. It has a complicated structure in terms of the eigenstates of the hamiltonian

$$H=\sum_i T_i+\tfrac{1}{2}\sum_{i\neq j}V_{ij} \tag{2.4}$$

of the nuclear system. The detailed form of $S(k,\omega)$ is not very useful for our purpose, but can be found in refs. [4-8]).

The real and imaginary parts of the Green function are linked by a dispersion relation

$$\mathrm{Re}\,\bar{G}(k,\omega)=\int_{-\infty}^{+\infty}\frac{\mathrm{d}\omega'}{2\pi}\frac{\mathscr{P}}{\omega-\omega'}\frac{\mathrm{Im}\,\bar{G}(k,\omega')}{\tanh\tfrac{1}{2}\beta\omega'}. \tag{2.5}$$

Important properties of the Green functions are

$$S(k,\omega)\geqslant 0, \tag{2.6}$$

$$\int_{-\infty}^{+\infty}\frac{\mathrm{d}\omega}{2\pi}S(k,\omega)=1, \tag{2.7}$$

$$\mathrm{sgn}\,(\mathrm{Im}\,\bar{G}(k,\omega))=-\mathrm{sgn}\,\omega, \tag{2.8}$$

$$\bar{G}(k,\omega)\to\frac{1}{\omega},\qquad |\omega|\to\infty. \tag{2.9}$$

The momentum distribution $\rho(k)$, normalized to unity, defined by

$$\rho(k)=\langle a_k^{\dagger}a_k\rangle, \tag{2.10}$$

is related to the Green function by

$$\rho(k)=-i\lim_{t\to 0^-}\int_{-\infty}^{+\infty}\bar{G}(k,\omega)\,\mathrm{e}^{-i\omega t}\frac{\mathrm{d}\omega}{2\pi}. \tag{2.11}$$

One has:

$$\int\frac{\mathrm{d}^3k}{(2\pi)^3}\rho(k)=1. \tag{2.12}$$

These formulae are those written down in all textbooks, but in the following, we will use the Green function $G(k,E)$ related to $\bar{G}(k,\omega)$ by

$$G(k,E)=\bar{G}(k,\omega-\mu), \tag{2.13}$$

in order to keep on with the usual definition at zero temperature [1]). Below, we will frequently refer to the mass operator $M(k, E)$ or self-energy defined by

$$G(k, E) = \frac{1}{E - k^2/2m - M(k, E)}. \tag{2.14}$$

The mass operator is complex and its analytical properties are similar to those of the Green function itself.

2.2. PERTURBATION SERIES

The most usual approach is to calculate the Green function by perturbation series. At nonzero temperature, the Green functions described above are not very suitable, since the perturbation series are not the same as at zero temperature. We already comment on this point in our previous work [3]). The reason is that Wick's theorem is not directly applicable at $T \neq 0$, which leads to many more diagrams. Let us notice that the differences come at the second order in the bare (or renormalized) interaction only. It is possible to remove all these additional diagrams by the introduction of the Matsubara Green functions [9]). They have different analytical properties [7,10]) and are not defined for all ω. This last feature is rather disturbing since many quantities we are interested in are defined for any ω and have at $T = 0$ particular properties linked to the continuous variation with ω. Hence, we choose to work with real time Green functions. As we will concentrate on general properties at low temperatures, the additional diagrams may be expected to be rather small. We will comment more specifically on some of them in the course of this work.

3. The mass operator

3.1. INTRODUCTION

Here we evaluate the mass operator $M(k, E)$ on the energy shell by means of Brueckner theory in the second order in the renormalized interaction. This leads us to a different definition of the self-consistency for the average field, as explained in sect. 3.2. In sect. 3.3, we describe our approximation scheme. We present our results for the calculation of the real and imaginary parts of the optical-model potential in sects 3.4 and 3.5, respectively. We compare our results with previous works in sect. 3.6. All the calculations below are performed at normal density $\rho = \rho_0 = 0.17\,\mathrm{fm}^{-3}$.

3.2. THE BRUECKNER SCHEME

For a detailed account of this scheme, we refer to review articles [11,1,12]). Here we just sketch the main points and elaborate on the new aspects of our work. As is

well known, the cornerstone of Brueckner approach is the resummation of the ladder diagrams to take account of the fact that the nuclear interaction is so strong that repeated interaction between two nucleons should be considered as the basic dynamical input of the theory. This is realized by rewriting the perturbation series in terms of bare interaction v as a series in terms of a renormalized interaction, the g-matrix, solution of the Bethe-Goldstone equation

$$g(w) = v + v \sum_{a,b} |\boldsymbol{a}\,\boldsymbol{b}\rangle \frac{Q(a,b)}{w - e(a) - e(b) + i\varepsilon} \langle \boldsymbol{a}\,\boldsymbol{b}| g(w) \,. \tag{3.1}$$

The Pauli operator Q is given by

$$Q(a,b) = (1 - n(a))(1 - n(b)) \,, \tag{3.2}$$

where $n(k)$ is the occupation probability of level k in the non-interacting case (the Boltzmann constant k_B is set equal to one)

$$n(k) = \left[1 + \exp\left(\frac{e(k) - \mu}{T} \right) \right]^{-1} . \tag{3.3}$$

The single-particle energy ($\hbar = 1$)

$$e(k) = \frac{k^2}{2m} + U(k) \tag{3.4}$$

includes an average field, which is usually determined by a self-consistency condition (see below).

In the Brueckner approach, one usually recasts the perturbation series into an expansion in terms of the number of hole lines in Goldstone diagrams [11]). For the mass operator (eq. (2.14)), this expansion may be written

$$M(k,E) = M_1(k,E) + M_2(k,E) + M_3(k,E) + M_4(k,E) + \cdots \,, \tag{3.5}$$

with

$$M_1(k,E) = \sum_j n(j) \langle \boldsymbol{k}\boldsymbol{j}| g[E + e(j)] |\widetilde{\boldsymbol{k}\boldsymbol{j}}\rangle \,, \tag{3.6}$$

$$M_2(k,E) = \tfrac{1}{2} \sum_j \sum_l \sum_a n(j) n(l) (1 - n(a)) \frac{|\langle \boldsymbol{j}\boldsymbol{l}| g[e(j) + e(l)] |\widetilde{\boldsymbol{k}\boldsymbol{a}}\rangle|^2}{E + e(a) - e(j) - e(l) - i\varepsilon} \,, \tag{3.7}$$

and

$$M_3(k,E) = \sum_j n(j) \langle \boldsymbol{k}\boldsymbol{j}| g[E + e(j)] |\widetilde{\boldsymbol{k}\boldsymbol{j}}\rangle [\rho_1(j) - 1] \,, \tag{3.8}$$

where $\rho_1(j)$ is an approximate value of $\rho(j)$ (eq. (2.10)), whose exact expression is defined later.

It is generally accepted nowadays that the auxiliary potential $U(k)$ is not merely a parameter, supposed to improve the convergence rate of (3.5), but should be chosen as to preserve the general analytic properties of $M(k,E)$ at any level of

approximation [13]) and to represent the physical properties of the mean field [14]). The so-called continuous choice fulfills these requirements and reads

$$e(k)=\frac{k^2}{2m}+\mathrm{Re}\, M_1(k, e(k))\,. \tag{3.9}$$

Since in this paper we want to go further in the perturbation series, we extend (3.9) to include the second-order term in eq. (3.5), i.e.

$$e(k)=\frac{k^2}{2m}+\mathrm{Re}\,[M_1(k, e(k))+M_2(k, e(k))]\,. \tag{3.10}$$

This choice, already made in ref. [13]), is not simply guided by symmetry reasons, but is more satisfactory from the physical point of view. Indeed, as we will see in sect. 3.5, it allows at $T=0$ to treat the mean field of particle and hole states on the same footing.

Furthermore, it is expected that the single-particle energy, i.e. the pole of the propagator (2.14) will be better approximated by solving eq. (3.10) rather than a similar equation, obtained by replacing $e(k)$ on the r.h.s. by any lower order approximation.

The mass operator is a complex quantity

$$M(k, E)=V(k, E)+iW(k, E)\,. \tag{3.11}$$

When evaluated on the energy shell ($E=e(k)$), this quantity can be considered as the optical-model potential. Its real and imaginary parts can be written

$$V(k)=V(k, e(k))=V_1(k)+V_2(k)+V_3(k)+\cdots, \tag{3.12a}$$

$$W(k)=W(k, e(k))=W_1(k)+W_2(k)+W_3(k)+\cdots, \tag{3.12b}$$

which reminds of the original perturbation series. Below, we will adopt the following notation

$$V_{\mathrm{po}}=V_1, \qquad W_{\mathrm{po}}=W_1, \qquad V_{\mathrm{co}}=V_2, \qquad W_{\mathrm{co}}=W_2\,. \tag{3.13}$$

According to the usual terminology V_{po} is called the polarization potential and V_{co} the correlation potential.

3.3. APPROXIMATION SCHEME

In principle, the g-matrix and the series (3.5) have to be calculated, starting from given values of temperature T and chemical potential μ. However, as indicated in our previous work [3]), the iterative procedure for solving the Bethe-Goldstone equation may then become unstable. For this reason, we use the baryon density ρ as an input and the unperturbed occupation probabilities are taken as

$$n(k)=\frac{1}{1+\exp\,[\beta(e(k)-\tilde{\mu})]}\,. \tag{3.14}$$

The normalization condition

$$\sum_k n(k) = \rho \tag{3.15}$$

determines the parameter $\tilde{\mu}$. The latter is an approximate value of the chemical potential, since eq. (3.15) cannot be true in general. The presence of the single-particle spectrum (3.10) in relation (3.14) forces a double self-consistency procedure in solving the Bethe–Goldstone equation.

The quantities M_1 and M_2 (eqs. (3.6), (3.7)) are calculated explicitly. The detail of the calculation of M_2 is contained in appendix A. The results shown below refer to the Paris potential [15]).

3.4. REAL PART OF THE OPTICAL-MODEL POTENTIAL

We present in fig. 1 the value of the real part of the optical-model potential in nuclear matter calculated at the second order in the g-matrix, i.e.

$$V(k) = V_{\rm po}(k) + V_{\rm co}(k)\,, \tag{3.16}$$

at zero temperature. We compare with the result (short-dashed curve) corresponding to the usual self-consistency requirement.

$$V(k) = V^{(0)}_{\rm po}(k) = \mathrm{Re}\, M_1(k, e^{(0)}(k))\,, \tag{3.17}$$

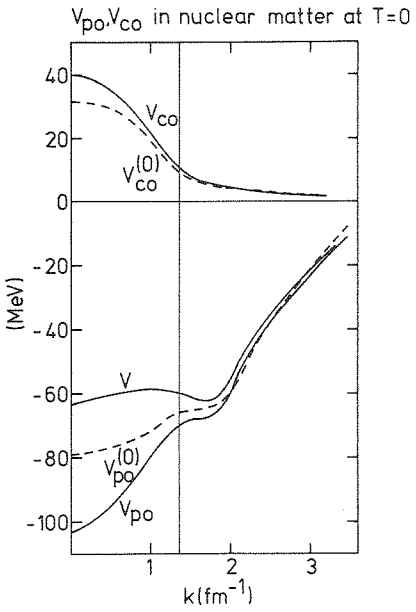

Fig. 1. Polarization ($V_{\rm po}$), correlation ($V_{\rm co}$) and total (V) single-particle potentials in cold nuclear matter at normal density, as calculated with the Paris potential and the self-consistency condition (3.10). The short-dashed line $V^{(0)}_{\rm po}$ gives the polarization potential when the usual continuous choice (3.9) is used. The short-dashed line $V^{(0)}_{\rm co}$ represents the first iteration of the correlation potential. See text for detail.

where $e^{(0)}(k)$ is solution of the eq. (3.9). Several interesting features arise from our results; (i) the polarization potential V_{po} deepens considerably below k_F, and especially at small k, when one goes from self-consistency condition (3.9) to condition (3.10); (ii) the correlation potential V_{co} is repulsive and essentially applies to states within the Fermi sea; (iii) the total potential $V(k)$ is less attractive when the correlation term is included - the reduction is of the order of 15 MeV.

The calculation of V_{po} and V_{co} has been performed iteratively in order to achieve self-consistency (3.10). We start with $V_{po}^{(0)}$, calculate $V_{co}^{(0)}$ (shown by the short dashes in fig. 1) by eq. (3.7) with the spectrum $e^{(0)}(k)$, recalculate this spectrum $e^{(1)}(k)$ by adding $V_{co}^{(0)}$ to $V_{po}^{(0)}$, recalculate $V_{po}^{(1)}$ by (3.6) with $e^{(1)}(k)$, recalculate $V_{co}^{(1)}$, etc. In this procedure, $V_{po}(V_{co})$ becomes gradually more attractive (repulsive). This can be understood by considering eqs. (3.6), (3.7) and the fact that the spectrum $e(k)$ is changing below the Fermi momentum k_F essentially. An average (over k) variation δV_{co} induces a variation δV_{po} which may be written as

$$\delta V_{po} \approx 2\left\langle \left.\frac{\partial M_1}{\partial E}\right|_{E=e(k)} \right\rangle \delta V_{co}\,, \tag{3.18}$$

where the brackets indicate the average over the Fermi sea. One thus have from the one iteration to the other

$$\delta V_{po}^{(n+1)} \approx 2\left\langle \left.\frac{\partial M_1}{\partial E}\right|_{E=e(k)} \right\rangle \delta V_{co}^{(n)}\,. \tag{3.19a}$$

Similarly, one has

$$\delta V_{co}^{(n+1)} \approx -\left\langle \left(\frac{\partial M_2}{\partial E}\right)_{E=e(k)} \right\rangle \delta V_{po}^{(n)}\,. \tag{3.19b}$$

In the average, $\partial M_1/\partial E$ and $\partial M_2/\partial E$ are negative (see sect. 4), which explains the observed variations in the numerical calculations. Eqs. (3.19) give semi-quantitatively the numerical values that we have obtained after iteration.

In fig. 2, we show the results for nonzero temperatures. As matter is heated, the correlation as well as the polarization potential decreases in magnitude. The resulting potential $V(k)$ is not changing very much and becomes slightly deeper. This may not be significant however. Indeed we have estimated M_3 and M_4 contributions through the following approximations:

$$M_3(k, E) \approx M_1(k, E)(\rho_1(\bar{j}) - 1)\,, \tag{3.20a}$$

$$M_4(k, E) \approx M_2(k, E)[(\rho_1(\bar{j}))^2 - 1]\,. \tag{3.20b}$$

In the first relation, which is an approximation of eq. (3.8) and in the second one, which is proposed in ref. [16]), $\bar{j}$ is the average value of momentum j calculated on the ρ_1 distribution (see sect. 5). Typically, $\bar{j} \approx \sqrt{0.6}k_F$. When the contributions (3.20) are added to M_1 and M_2, one obtains a potential $V(k)$ as in fig. 3. It should be noticed that these contributions are sizeable. For small k, M_3 and M_4 are of the

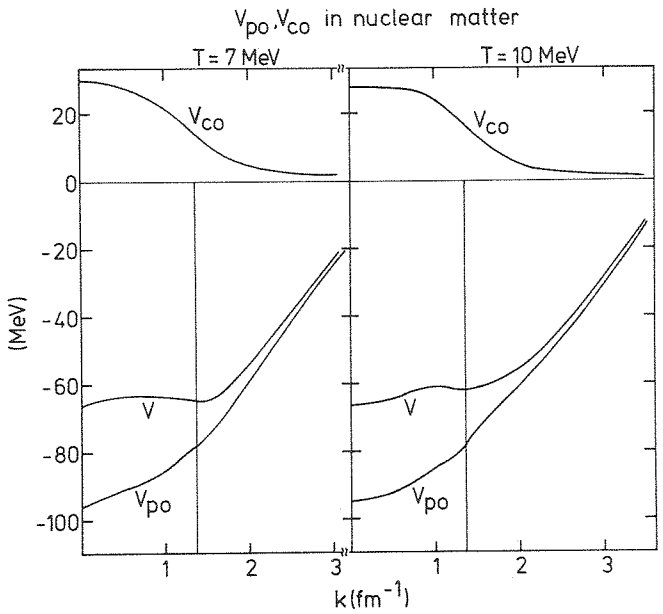

Fig. 2. Polarization (V_{po}), correlation (V_{co}) and total (V) single-particle potential at $T = 7$ and 10 MeV.

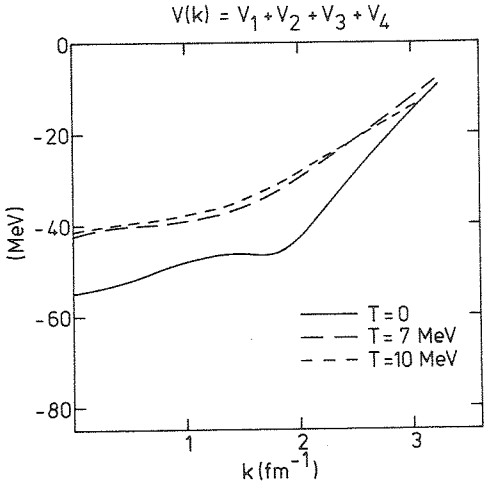

Fig. 3. Single-particle potential including third and fourth hole line corrections (see text).

order of 5–10 MeV, with opposite signs. The magnitude of M_3 and M_4 may cast some doubt about the convergence of the series (3.5). However, these approximations may not be reliable and are shown here for completeness. Even with M_1 and M_2, we achieve an improvement as compared to the usual M_1 approximation of the real part of the optical-model potential. Indeed, the experimental values (in nuclei) are

closer to 60 MeV than 80 MeV for deep lying states [17]) (in cold nuclei). A similar conclusion is obtained in ref. [25]).

3.5. IMAGINARY PART OF THE OPTICAL-MODEL POTENTIAL

In fig. 4, we give the imaginary part $W_{po}(k)$ and $V_{co}(k)$ (see eq. (3.12)) of the optical-model potential, for cold as well as heated nuclear matter. The quantity Im $W_{po}(k)$ is negative, while Im $W_{co}(k)$ is positive. The graphs of fig. 5 indicate that the imaginary part of W_{co} refers to the width (and the lifetime) of a hole state. Similarly, Im W_{po} corresponds to particle states. As can be seen from fig. 4, the

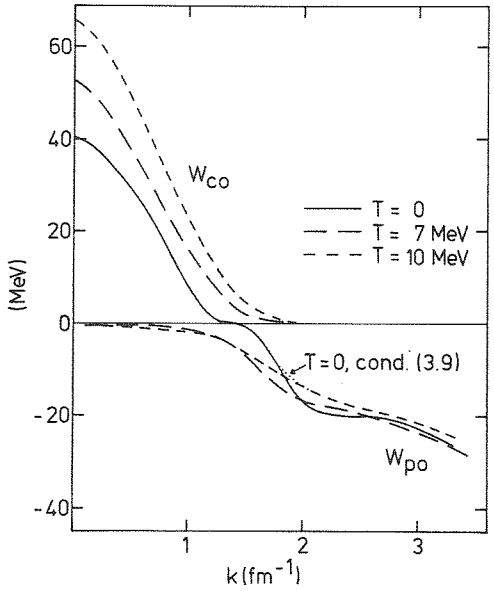

Fig. 4. Polarization and correlation contributions to the imaginary part of the single-particle energy. Self-consistency condition (3.10) is used. The dotted curve corresponds to the imaginary part at $T=0$, when self-consistency condition (3.9) is adopted. It is explicitly shown wherever it differs from the full line or the dashed line only.

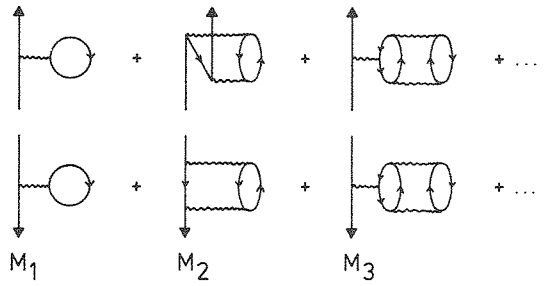

Fig. 5. First order contributions to particle (upper row) and to hole (lower row) self-energy.

imaginary part of the correlation potential is quite important in the bottom of the Fermi sea. Fig. 4 also shows that when going from the ordinary self-consistency requirement (3.9) to requirement (3.10), the absorptive potential increases somewhat. The temperature dependence of $W_{po}(k)$ is similar to the one obtained in our previous work [3]). The quantity $W_{co}(k)$ does show a stronger temperature dependence. We also see that the tail extends above k_F, which is a trivially expected effect. It is interesting to note that $W(k)$ exhibits a zero close to k_F for the two temperatures shown in fig. 4. This is consistent with eqs. (2.8), (2.13), since the quantity $\tilde{\mu}$ (roughly the chemical potential) does not change very much between $T=0$ and 10 MeV (see table 1).

3.6 COMPARISON WITH PREVIOUS WORKS

The previous calculations of the correlation graph are rather scarce. The oldest and quite schematic calculations have been done by Brueckner and co-workers [18-19]). Köhler [20]) has performed a microscopic calculation using the Brueckner-Gammel potential and the standard choice ($U(k)=0$ for $k>k_F$) for the single-particle spectrum. More elaborate calculations have been done by Sartor using however the semi-realistic Hamman-Ho Kim potential, with the self-consistency requirement (3.9) [ref. [21])] as well as with (3.10) [ref. [13])]. The correlation graph off the energy shell ($E \neq e(k)$) has been calculated by Sartor and Mahaux [22]) for the dilute hard-sphere Fermi gas, by Bernard and Mahaux [23]) for a model s-wave interaction and by Orland and Schaeffer [24]) using the free scattering matrix and the Fermi-gas phase space approximation. More recently, Hasse and Schuck [25]) have looked at the problem. Yet, they use an effective gaussian interaction. The last four works also calculate the imaginary part of the correlation graph.

As for the real part V_{co}, our results are very close to those obtained by Köhler and by Sartor with the semi-realistic interaction. This could lead us to believe that the value of V_{co} (eq. (3.7)) is largely dominated by phase space considerations. This however partly contradicts our discussion of sect. 3.4, which concludes that the energy denominators play an important role, and the results of ref. [24]), which yields a very small value (~4 MeV) for V_{co}. Furthermore, the value obtained for the hard sphere gas [22]) is almost an order of magnitude smaller than ours. The model calculation of ref. [23]) concentrates on the region $k \approx k_F$, for which a value of around half of our prediction is obtained. Finally, the authors of refs. [24,25]) are able to make predictions for the value $V_{co}(k) - V_{co}(k_F)$ only, since they look for corrections to the Hartree-Fock field using a subtracted dispersion relation. Concerning this relative quantity, there is a gross agreement between ref. [25]) and our work and, as we just said above, a strong disagreement between ref. [24]) and our results. The difference between results of ref. [24]) and ref. [25]) should be due to the effective interaction. Comparing fig. 1 with ref. [25]), we notice that the shape of $V_{co}(k)$ is not the same and that the maximum value (at $k=0$) is ~40% smaller than in our case.

Also, in ref. [24]) as well as in ref. [25]), $V_{co}(k_F) = V_{co}(\infty) = 0$. This indicates that the correlation potential calculated in ref. [25]) is not directly comparable with ours. Indeed the two calculations are rather different in their premises. Ours is a purely microscopic calculation based on a realistic two-body interaction, while ref. [25]) aims at calculating a correction to the Hartree–Fock field with the help of a phenomenological interaction, which, alone, cannot lead to saturation, and which reproduces, in the Hartree–Fock picture, quantities like binding energy, radii, separation energies, etc. . . . , that already contain some correlation effects while the latter are precisely the aim of the calculation. Furthermore, our calculation incorporates a fully self-consistent single-particle spectrum. In addition it seems that results of ref. [25]) are quite sensitive to the range of the effective interaction. This comparison deserves to be cleared up. In conclusion, all the ambiguities linked with the use of an effective interaction are removed in our approach.

Concerning the imaginary part W_{co}, our results are very close to Sartor's calculation. Our calculation shows that this quantity possesses a strong temperature dependence. Let us finally note that comparing our results with those of Bernard and Mahaux [23]) (for $W_{co}(k_F, E)$) reveals that off-shell effects are quite important.

4. The effective mass

4.1. INTRODUCTION

The effective mass appears as an important quantity in relation with various phenomena like the density of states close to the Fermi level [26]), the imaginary potential [27]), the coupling to surface vibrations [28-29]), the giant resonances themselves [30]), and even nuclear transport theory in general [31-32]). It is defined by ($m = 1$)

$$m^* = \frac{k}{\mathrm{d}e(k)/\mathrm{d}k}. \tag{4.1}$$

Physically, it represents the ratio of the momentum of the particle to the (group) velocity of its wave packet and is related to the mass operator through the relation

$$m^* = \left[1 + \frac{1}{k}\frac{\mathrm{d}}{\mathrm{d}k}\,\mathrm{Re}\,M(k, e(k))\right]^{-1} \tag{4.2}$$

and to the k- and E-dependences of the mass operator by [33,1])

$$m^* = \tilde{m}\tilde{m}, \tag{4.3}$$

where

$$\bar{m} = 1 - \frac{\partial}{\partial E}\,\mathrm{Re}\,M(k, E)\bigg|_{E=e(k)} \tag{4.4}$$

and

$$\tilde{m} = \left[1 + \frac{1}{k}\frac{\partial}{\partial k}\,\mathrm{Re}\,M(k, E)\bigg|_{E=e(k)}\right]^{-1}. \tag{4.5}$$

4.2. RESULTS

We report in fig. 6 on our calculation of m^*, when the mass operator is calculated to the second order (in g) and with the self-consistency requirement (3.10). The most important feature is the peak located close to k_F at zero temperature. Historically, the existence of such a peak was conjectured in ref. [26]) and verified on an explicit calculation with a semi-realistic interaction in ref. [13]). This property was also checked on model calculations [22,23]). Finally, it was deduced in ref. [34]) from the phenomenology of the optical-model potential for finite nuclei. For the latter case, the peak may have another origin from the one in nuclear matter. In our calculation, the effective mass peaks to a value of around 1.15*,, close to values quoted in refs. [26,34]). The width of the peak is also consistent with what is suggested in ref. [26]), with model calculation predictions [22,23]) and with the phenomenology of finite nuclei [34]).

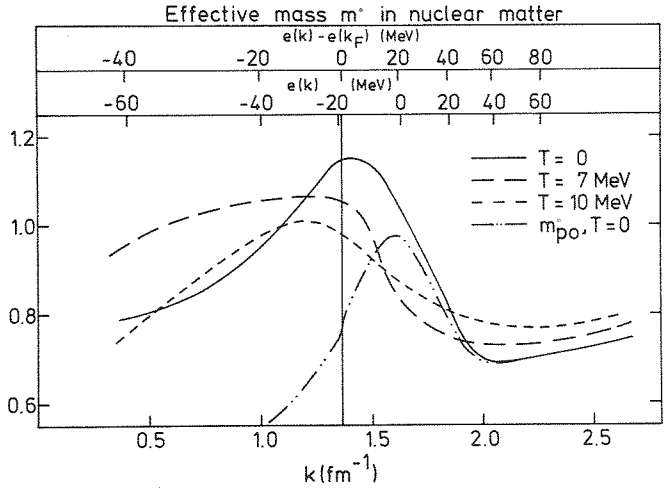

Fig. 6. Nucleon effective mass eq. (4.6) at various temperatures. The curve with double dots and dashes indicates the effective mass calculated with the polarization potential only.

When only the core-polarization contribution (M_1) is taken into account, with either the ordinary self-consistency condition (3.9) (see ref. [3])) or condition (3.10) (see fig. 6), the enhancement of m^* lies above the Fermi level. The correlation contribution drives the enhancement toward k_F. To our knowledge, there is no theoretical indication for having this maximum at precisely k_F, nor for having a symmetrical peak.

When the effective mass is calculated with the polarization field only, with the self-consistency condition (3.9) (see ref. [3])) or with condition (3.10) (see fig. 6), it

* The calculation of m^* involving a numerical derivative of the spectrum $e(k)$ (see eq. (4.1)), it has a limited accuracy, which we estimate to be of the order of 0.05.

exhibits a peak which is due to the wiggle appearing in the V_{po} curve around k_F. Physically, this peak arises from the excitation of the so-called core-polarization states, whose density sharply increases above the Fermi energy. When the matter is heated up these core-polarization states are more and more spread out and the wiggle disappears. With the help of eqs. (4.2), (3.11) and (3.16), one has, up to second order

$$m^* = \left[1 + \frac{1}{k}\left(\frac{dV_{po}}{dk} + \frac{dV_{co}}{dk}\right)\right]^{-1}. \tag{4.6}$$

Around k_F, the derivative V_{po}/dk rapidly decreases as T goes up. This, alone, would make $m^*(\sim k_F)$ strongly decreasing. The quantity $dV_{co/dk}$ is, on the contrary, fairly constant around k_F, when T increases. As a consequence, $m^*(\sim k_F)$ decreases much more slowly than it does when the correlation graph is left out [3]).

The value of m^* for $k \ll k_F$ is largely dominated by the roughly parabolic behaviour of V_{po} and V_{co} in this region. Grossly speaking, V_{co} and V_{po} remain quadratic for $k < 1$ fm^{-1} as T increases. Taking the curvatures of potential curves (see figs. 1 and 2), one gets by this rough estimate $m^* \approx 0.8$ for $T = 0$ and $m^* \approx 0.95$ for $T = 7$ MeV. Such a modification of $V_{po}(k)$ for small k was not observed in our previous work, where we used condition (3.9). This led us to believe that the broad shoulder in m^* is largely an effect of the self-consistency. Therefore, it is hard to ascribe it a precise physical nature.

Our value for $m^*(k = k_F)$ at zero temperature ($\sim$1.15, in the $M_1 + M_2$ approximation) is notably larger than the values ($\sim$0.8) quoted in refs. [35,25,36]) and than the "experimental" value ($\sim$0.85) at the centre of the Pb nucleus [37]). This difference may come from the self-consistency scheme and/or from the interaction used. Eqs. (4.1) and (2.14) suggest that calculating the mass operator with the self-consistency (3.10) should be favoured for the calculation of the effective mass. Doing so, one increases (with respect to the usual condition (3.9)) the wound integral κ (see sect. 5 and fig. 9), probably worsening at the same time the convergence of the hole line series [38]). It is then not surprising that including the M_3 and M_4 contributions makes $m^*(k_F)$ closer to the value of ref. [35]). Anticipating on sect. 4.3, one can realize from eqs. (3.20) that inclusion of M_3 and M_4 decreases the quantities $\bar{m}_1$ and $\bar{m}_2$, and henceforth $\bar{m}$ (in eq. (4.7a)). Since $\tilde{m}$ is largely independent of any self-consistency scheme, m^* will be decreased, owing to eq. (4.3), when M_3 and M_4 are taken into account. With our numerical values, we find that $\bar{m}(k_F)$ becomes $\approx$1.45 and, consequently, $m^*(k_F)$ becomes $\approx$0.95. The remaining difference between this value and the one of ref. [35]) can most probably be attributed to the specificity of the Paris potential (this appears consistent with our earlier result of ref. [3]) where we already found a maximum value of 0.9 for m^*, considering the polarization contribution only). This question need however be clarified and is presently under investigation. Taking account of this possible interaction effect, one can reasonably conclude, that, to a large extent, the hole line expansion up to M_4 is in fair agreement with

the so-called CBF theory [35]), at least for "hard" potentials, i.e. those giving a large κ-value.

4.3. THE *E*-MASS

It is interesting to look at the energy mass $\bar{m}$, which comes from the genuine energy dependence of the effective interaction (4.2). It carries the simplest information about the off-shell properties of the mass operator. In fig. 7, we give the value of $\bar{m}$ calculated at the second order in g:

$$\bar{m} = \bar{m}_1 + \bar{m}_2 , \tag{4.7a}$$

$$\bar{m}_1 = 1 - \frac{\partial}{\partial E} \operatorname{Re} M_1(k, E)\Big|_{E=e(k)} , \tag{4.7b}$$

$$\bar{m}_2 = -\frac{\partial}{\partial E} \operatorname{Re} M_2(k\,E)\Big|_{E=e(k)} . \tag{4.7c}$$

The quantity $\bar{m}_2$ is positive, as can be checked from eq. (3.7). The same is true [1]) for $\bar{m}_1 - 1$. These properties are directly responsible for the variations of V_{co} and

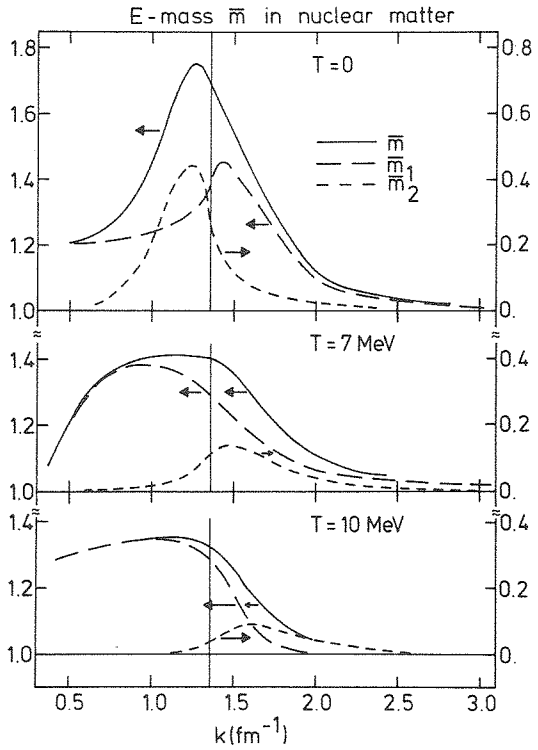

Fig. 7. Energy mass $\bar{m}_1$ (long dashes), $\bar{m}_2$ (short dashes) (eq. (4.7)) and their sum $\bar{m}$ (full curves) for several temperatures.

V_{po} from one iteration of their calculation to the other, as mentioned in sect. 3.4. Similarly to the results of refs. [21-23]), our calculation predicts a peak in $\bar{m}_1$ above k_F and a peak in $\bar{m}_2$ below k_F at $T=0$. Both $\bar{m}_1$ and $\bar{m}_2$ possess an infinite derivative at $k=k_F$. Let us notice that $\bar{m}_1$ has a plateau at $k<k_F$ for a value $\bar{m}_1 \approx 1.2$.

A somewhat unexpected result shows up in the temperature dependence of $\bar{m}_1$ and $\bar{m}_2$. At $T=7$ MeV, the peak in $\bar{m}_1$ has completely disappeared. On the other hand the plateau below k_F has risen a little bit. As a consequence a large bump appears below k_F. The peak of $\bar{m}_2$ below k_F has also collapsed and the tail above k_F has transformed into a little bump. At 10 MeV, the tendency is accentuated for $\bar{m}_2$, but the bump in $\bar{m}_1$ has decreased.

The collapse of the peak $\bar{m}_1$ (or $\bar{m}_2$) is not really surprising. For a long time [1]), it has been recognized that a sudden rise in the imaginary part W_{po} close to the threshold of real excitations (k_F at $T=0$) gives a wiggle in V_{po} and a peak in $\bar{m}_1$. The two quantities V_{po} and W_{po} are linked by the dispersion relation at $T=0$

$$\text{Re } M_1(k, E) = \frac{\mathscr{P}}{\pi} \int_{e(k_F)}^{\infty} \frac{\text{Im } W_1(k, E')}{E - E'} \, dE' . \tag{4.8}$$

Similarly, the quantity $\bar{m}_2$ shows a maximum below k_F because W_{co} increases rapidly below k_F [ref. [23])]. When T increases, the sudden rise or the threshold effects in Im W_1 and Im W_2 are rapidly washed out, as indicated by fig. 4 and by fig. 3 of ref. [3]). The only surprising result is in fact the rise in the plateau of $\bar{m}_1$ below k_F. We are, however, confident in the accuracy of our calculation. Indeed, m^* can be obtained directly through eq. (4.6) or indirectly through eqs. (4.3)-(4.5) and (4.7a). We did not calculate $\tilde{m}$, but this quantity is a smooth function of k [ref. [1])]. Therefore the structure of m^* should follow the structure of $\bar{m}$. Observation of figs. 6 and 7 shows they are clearly consistent with each other, despite the independent calculation of m^* and $\bar{m}$ and despite the lesser numerical accuracy of the calculation shown in fig. 6.

4.4. THE LEVEL DENSITY PARAMETER

In ref. [3]), we have already paid some attention to the relationship between the effective mass and the level density parameter. Strictly speaking, the latter quantity is the coefficient of T^2 in the low temperature expansion of the internal energy (at fixed density)

$$\frac{U}{A}(T) = \frac{U}{A}(0) + \frac{a}{A} T^2 + \cdots . \tag{4.9}$$

The coefficient a coming from the expansion of the usual (Brueckner)-Hartree-Fock approximation

$$\frac{U}{A} = \frac{1}{\rho} \frac{\nu}{2\pi^2} \int_0^{\infty} dk \, k^2 n(k) \left[\frac{k^2}{2m} + V(k) \right] \tag{4.10}$$

is given by

$$\frac{a}{A}=\frac{1}{3\rho}k_{\mathrm{F}}\frac{m^*(m^*+1)}{2}, \tag{4.11}$$

where m^* is the effective mass at k_{F} and $T=0$. This result is readily obtained by using the Sommerfeld expansion of the Fermi distribution $n(k)$, by taking into account in lowest order the variation of μ with temperature, and by neglecting the temperature variation of $V(k)$ and the derivative $\mathrm{d}m^*/\mathrm{d}k$ close to k_{F}. Expression (4.11) differs from eq. (5.9) of ref. [3]), because therein the variation of the chemical potential is neglected. The Sommerfeld expansion of $n(k)$ alone would give an expansion of U of the form:

$$\frac{U}{A}=\frac{U_0(T)}{A}+\frac{\tilde{a}(T)}{A}T^2+\cdots, \tag{4.12}$$

where*

$$\frac{\tilde{a}(T)}{A}=\frac{1}{3\rho}\left[\frac{m^*}{2}k(1+2m^*)+\frac{m^{*2}}{k}V(k)\right]_{k=k(\mu)}. \tag{4.13}$$

In ref. [3]) this expression is written down incorrectly. Therein, a factor 2 should be removed from the first term in the r.h.s. of eq. (5.9). The quantity $U_0(T)$ depends upon T through the chemical potential μ and through a possible variation of $V(k)$ with temperature. Taking account of the first effect (in lowest order only), one may rewrite the first two terms of eq. (4.12) as

$$\frac{U}{A}(T)\approx\frac{U}{A}(0)+\frac{a^*(T)}{A}T^2, \tag{4.14}$$

with

$$\frac{a^*(T)}{A}=\frac{1}{3\rho}k\frac{m^*(1+m^*)}{2}\bigg|_{k=k(\mu(T))}. \tag{4.15}$$

An expression like (4.14) has been recently used in experimental studies [39]) which aimed to look at the temperature dependence of the "apparent"** level density parameter. The same problem has been studied theoretically in refs. [40,41]). Our numerical values of m^*, which decreases with temperature, as well as $k(\mu)$, are in favour of the conjecture that the observed decrease of $a^*(T)$ with increasing temperature is due to the decrease of $m^*(k(\mu))$. Presently, this is only a conjecture, since surface effects [42]) and collective excitations [36]) could change the effective mass sizeably. In our case, the variation of $V(k)$ with temperature makes expressions (4.14), with (4.15), rather different from the actual values of $\frac{U}{A}(T)$. In other words,

* Here, a term containing a factor $\mathrm{d}m^*/\mathrm{d}k$ at $k=k(\mu)$ has been neglected.

** Such an analysis [39]) concentrates on the relationship between U and T and is not directly related to level density.

fitting our numerical values of $\frac{U}{A}(T)$ with an expression like (4.14) for $T = 0$–10 MeV, gives an average value of a^* quite smaller than the phenomenological value of a in nuclei and even smaller than the Hartree-Fock value with effective forces.

5. The momentum distribution

The momentum distribution $\rho(k)$ (eq. (2.10)) can be calculated perturbatively, e.g. by introducing the perturbative series (3.5) in eqs. (2.14), (2.13) and (2.11). As explained in ref. [43]), the perturbation series can also be obtained by drawing diagrams for a one-body operator. In the Brueckner approach at $T \neq 0$, one obtains up to second order in the g-matrix, the diagrams shown in fig. 8. The first line, which contains the diagrams present at $T = 0$, may be rewritten as

$$\rho(k) = \rho_1(k) + \rho_2(k) , \tag{5.1}$$

with

$$\rho_1(k) = n(k)[2 - \bar{m}_1] , \tag{5.2}$$

and

$$\rho_2(k) = (1 - n(k))\bar{m}_2 , \tag{5.3}$$

where $\bar{m}_1$ and $\bar{m}_2$ are defined in eq. (4.7). The diagrams of the last line (fig. 8) do not exist at $T = 0$. They are allowed at $T \neq 0$, because a level may be occupied and non-occupied at the same time. They however exactly cancel each other, in contradistinction to the corresponding diagram in the perturbative series of the free energy [see ref. [43]), for a discussion]. The contribution of the latter is proportional to T^2 and be crudely estimated to be ~ 0.02–$0.03\ T^2$.

It is attractive to interpret eq. (5.2) as describing the depopulation due to the M_1 term and eq. (5.3) to the population coming from the M_2 term. At $T = 0$ the depopulation is restricted below k_F and the population above k_F only. At finite temperature, these boundaries are no longer strict.

The results of our calculation for the quantity $\rho(k)$ (eq. (5.1)) are given by the full curve in fig. 9, for $T = 0$. We obtain the characteristic shape, with the infinite derivatives of $\rho(k)$ when k tends to k_F from above and from below. One notices

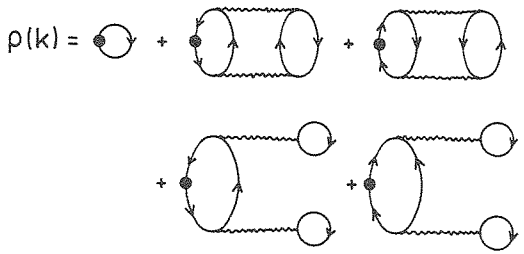

Fig. 8. Lowest order diagrams for the momentum distribution $\rho(k)$.

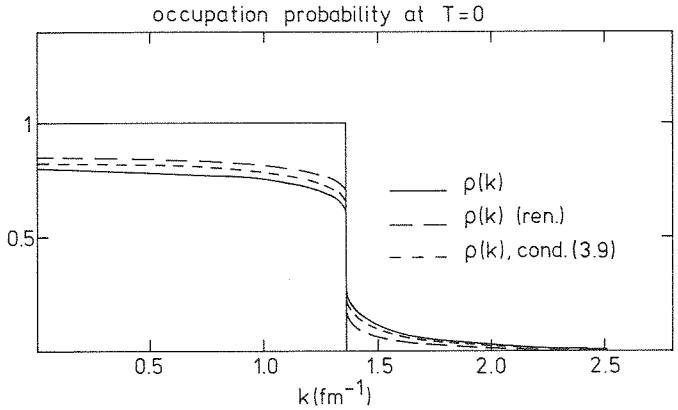

Fig. 9. Momentum distribution $\rho(k)$ (eq. (5.1)) for cold nuclear matter (full curve). The short-dashed curve represents $\rho(k)$ (eq. (5.1)) when the self-consistency condition (3.9) is used. The long-dashed curve corresponds to the momentum distribution when correction due to the M_3 and M_4 contributions is applied (see text for detail).

that the depletion of the Fermi sea is quite important. To fix the ideas, the parameter κ which can be defined as

$$\kappa = 1 - \rho(\bar{k}) \tag{5.4}$$

(where $\bar{k}$ is defined in sect. 3.4), is ~0.25, which seems to be a typical value for all very repulsive (hard core) potentials [38]) in the Brueckner approximation. The variational calculation of $\rho(k)$, made by Fantoni and Pandharipande [35]), using the v_{14} interaction, yields a much smaller value, although it is pointed out that the tensor correlations may bring κ up to ~0.18. It should be noticed that the results are sensitive to the self-consistency requirement. In fig. 9, we show the quantity (5.1) when condition (3.9) is used. This effect was already pointed out by Sartor [21]), although the sensitivity turns out to be larger for the Hamman-Ho Kim potential.

The discontinuity at k_F is related to the E-mass. In our $(M_1 + M_2)$ approximation, it is easily verified that

$$\rho(k_F^-) - \rho(k_F^+) = 1 + [1 - \bar{m}_1(k_F) - \bar{m}_2(k_F)] , \tag{5.5}$$

which appears as an approximation to the exact relation [44])

$$\rho(k_F^-) - \rho(k_F^+) = \frac{1}{\bar{m}(k_F)} . \tag{5.6}$$

We find $\rho(k_F^-) - \rho(k_F^+) \approx 0.35$, which is half as large as the value found in ref. [35]), including tensor correlations. Our value is very close to Sartor's one [13]), for the same self-consistency scheme (eq. (3.10)). With the usual self-consistency (3.9) we find $\rho(k_F^-) - \rho(k_F^+) \approx 0.5$ whereas the author of ref. [13]) finds ≈0.70, close to the value of ref. [35]). This seems to indicate that the quenching of the discontinuity in $\rho(k) = \rho_1 + \rho_2$ (eq. (5.1)) is partly due to a self-consistency effect. Therefore, if one uses

self-consistency (3.10), the contributions of M_3 and M_4 become important and should be included. As fig. 9 shows, the discontinuity then increases up to ~0.60. If on the other hand, self-consistency (3.9) is used, the discontinuity in $\rho_1+\rho_2$ is larger (see fig. 9 and ref. [13])), and the corresponding contributions of M_3 and M_4 are decreased, due to eqs. (3.20). The resulting discontinuity would be about the same as above. This raises the question of choosing the proper self-consistency scheme in the expansion series for $\rho(k)$: the choice which gives the fastest convergence of the expansion of $\rho(k)$ is not necessarily the one which might be advocated for the expansion of other quantities like B/A, $M(k, E)$, ...

We analyse the tail of the momentum distribution in fig. 10. Much interest has been devoted recently to this quantity, especially in finite nuclei [45-47]). We observe that the distribution $\rho(k)$ seems to be exponentially decreasing for $k \geqslant 2\ \mathrm{fm}^{-1}$, with the following form

$$\rho(k) \approx 0.9123 \exp(-k/0.5662\ \mathrm{fm}^{-1}) . \tag{5.7}$$

However, in the same interval ($2 \leqslant k \leqslant 2.8\ \mathrm{fm}^{-1}$), one cannot exclude a power law

$$\rho(k) \propto k^{-\alpha} , \tag{5.8}$$

where α is between 4 and 5. One cannot distinguish easily between the two forms because the interval is rather narrow. There is no theoretical argument to prefer one form to the other. The only condition is that $\rho(k)$ should decrease [22]) faster than k^{-4}. To our knowledge, there is no example, even on a model, of an exponential

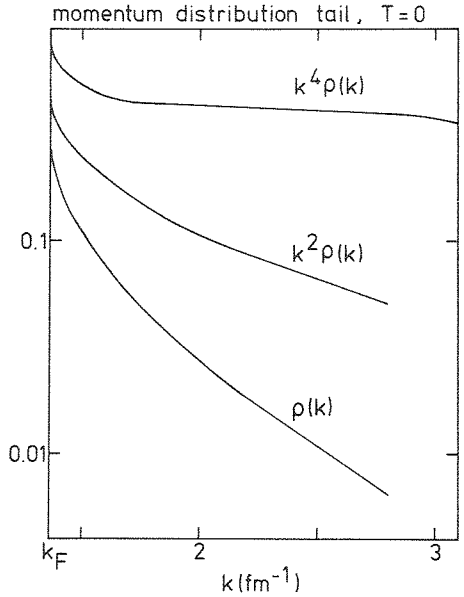

Fig. 10. Tail of the momentum distribution (eq. (5.1)) for cold nuclear matter. Also shown are the curves obtained after multiplication by k^2 and k^4.

tail for $\rho(k)$ in an infinite system. In a finite system of non-interacting fermions, such a tail seems to come from the analytical properties of the average potential [45]).

Fig. 10 also shows that there is no maximum in $k^2\rho(k)$ in contradiction to a conjecture by Day [48]), nor in $k^4\rho(k)$, which however exhibits a plateau between 2 and 3 fm^{-1}. This plateau is indicative of the maximum which would occur around 2.2 fm^{-1} if expression (5.7) was correct everywhere above k_F.

We believe that an exponential fall-off is more likely than an inverse power law in our case. Indeed, the normalization of $\rho(k)$ up to 2.8 fm^{-1} amounts to 0.96. When expression (5.7) is assumed beyond 2.8 fm^{-1}, the total normalization reaches unity within less than 1%. If eq. (5.8) is assumed, with $\alpha \leq 5$, the total normalization is

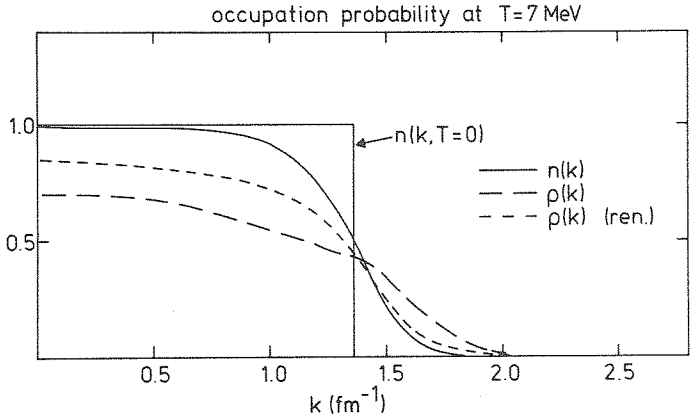

Fig. 11. Momentum distribution $\rho(k)$ (eq. (5.1)) for nuclear matter at 7 MeV temperature (long dashes). The short-dashed curve represents the distribution when correction due to M_3 and M_4 is applied. The full curve corresponds to the unperturbed distribution $n(k)$ (eq. (3.3)). The same quantity at $T=0$ is displayed for comparison.

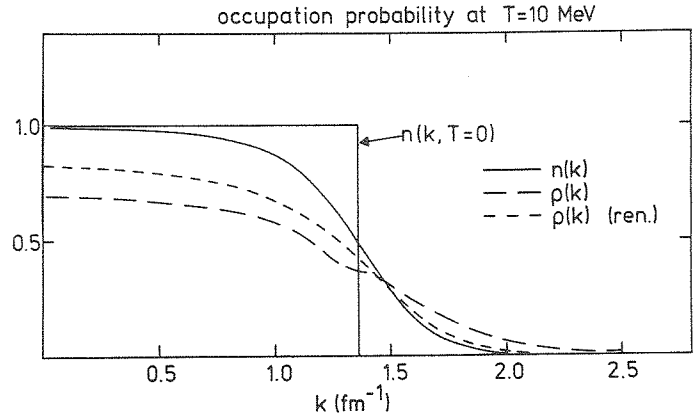

Fig. 12. Same as fig. 11 for $T=10$ MeV.

$\geqslant 1.035$. We recall that the normalization of $\rho(k)$ should be one, irrespective of the g-matrix. This also holds at finite temperature.

In figs. 11 and 12, we report on the calculation of the same quantity $\rho(k)$ for finite temperatures. The perhaps surprising feature is the fact that the depopulation for small values of k is larger at 7 MeV compared to $T=0$, but this follows automatically from the properties of the E-masses (see sect. 4.2). The wiggle around k_F comes from the continuous variation of ρ_1 and ρ_2. The final distribution $\rho(k)$ appears (close to the chemical potential) as a Fermi distribution with a much larger apparent temperature. We don't know whether this could have observable consequences. In figs. 11 and 12, we show, for illustrative purpose, the distribution corrected for the M_3 and M_4 contributions.

6. The spectral function

The spectral function is related to the mass operator at $T=0$ through eqs. (2.3), (2.13), (2.14), and (3.11):

$$S(k, E)=\frac{1}{\pi}\frac{W(k, E)}{[E-k^2/2m-V(k, E)]^2+[W(k, E)]^2}. \tag{6.1}$$

Roughly speaking, this function describes the spreading of a single-particle state. The simplest expression which neglects the energy dependence of the mass operator gives

$$S(k, E)=\frac{1}{\pi}\frac{\Gamma_0}{[E-e(k)]^2+\Gamma_0^2}, \tag{6.2}$$

with

$$\Gamma_0=W(k, e(k)). \tag{6.3}$$

It has been emphasized in the past [13,21,24]) that the energy dependence of V and W plays an important role. If the latter is restricted to a linear approximation both for V and W, one obtains

$$S(k, E)=\frac{1}{\pi}\frac{\Gamma_0+(E-e(k))\bar{m}_W}{(E-e(k))^2\bar{m}^2+[\Gamma_0+(E-e(k))\bar{m}_W]^2} \tag{6.4}$$

where $\bar{m}$ is defined in sect. 4 and where $\bar{m}_W$ is

$$\bar{m}_W=\frac{\partial W}{\partial E}(k, E)\bigg|_{E=e(k)}. \tag{6.5}$$

Expression (6.4) presents some interest in cases where the full E-dependence cannot be calculated as in our case (due to the complexity of the calculation). Furthermore, it displays qualitative effects of the E-dependence.

In fig. 13, we give our calculated values of $S(k, E)$ for a typical case, $T=0$, $\rho=\rho_0$, $k=0.55\,k_F$. The energy dependence of $V(k, E)$, responsible for the difference

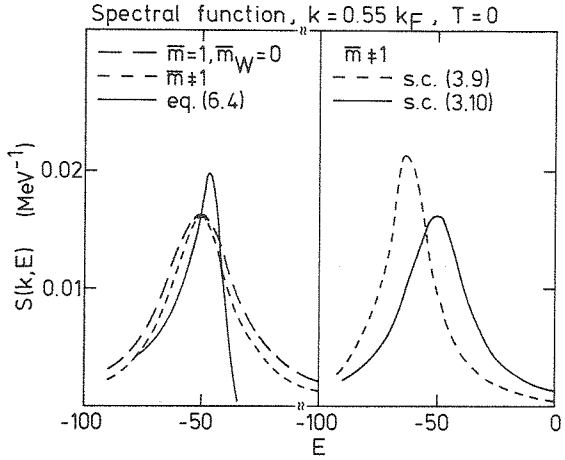

Fig. 13. Spectral function $S(k, E)$ for a hole state ($k = 0.55\ k_F$) in cold nuclear matter ($\rho = \rho_0$). Left side: approximations (6.1) (long dashes), (6.4) without $\bar{m}_W$ (short dashes) and with $\bar{m}_W$ (full curve). All these curves correspond to the single-particle spectrum $e(k)$ (in eq. (3.10)). Right side: approximation (6.4) without $\bar{m}_W$, and with self-consistency requirements (3.9) (short dashes) and (3.10) (full curve).

between the dashed curve (eq. (6.2)) and the dotted curve (eq. (6.4), with $\bar{m}_W = 0$) on the left, narrows the peak in the spectral function. The introduction of $\bar{m}_W$ (see full curve, eq. (6.4)) brings substantial modifications: the peak is shifted towards larger energies, narrowed and asymmetric. Of course, eq. (6.4) cannot be true for large $|E - e(k)|$, since there eq. (2.6) is violated. However, the E-dependence of $W(k, E)$ cannot be neglected for the calculation of the lifetime of hole states. In our case, $\bar{m}_W$ which refers to the correlation contribution only, goes from 0 at the top of the Fermi sea to ~3 at the bottom.

On the right of fig. 13, we show the effect of the self-consistency, but neglecting $\bar{m}_W$ in eq. (6.4). The passage from self-consistency (3.9) to self-consistency (3.10) has two effects: the peak energy is raised from −63 MeV to −51 MeV and the width is increased. These modifications were already noticed in ref. [21]).

7. Conserving approximations

We mentioned in ref. [3]) and in sect. 3.3, that the so-called Brueckner-Hartree-Fock approximation is nonconserving. In particular, the so-called Hugenholtz-Van Hove theorem [49]), which for finite temperature can be stated as

$$\mu = \frac{F}{A}, \tag{7.1}$$

where F is the free energy, is badly violated. Expression (7.1) should be considered at the saturation point. Even though we did not calculate a saturation curve for the $M_1 + M_2$ approximation with self-consistency (3.10), we can however be sure that the latter is much better conserving that the M_1 approximation with (3.9). Indeed

outside the saturation point, eq. (7.1) should be replaced by

$$\mu = \frac{F}{A} + \frac{p}{\rho}, \tag{7.2}$$

where p is the pressure. The latter will not change sizeably when going from one approximation to the other. At $\rho \approx \rho_0$ and $T = 0$ for the Paris potential, we obtained in ref. [3]) $p = -0.5$ MeV $\cdot$ fm^{-3}. Although the other approximation may change it by 50%, the argument below will be qualitatively valid. Around $\rho \approx \rho_0$, $p/\rho \approx -(4\text{-}6)$ MeV for $T = 0$, and $\approx -(2\text{-}3)$ MeV at $T = 10$ MeV. One can see from table 1 that expression (7.2) is well fulfilled in our approximation, whereas it is badly violated in the Brueckner-Hartree-Fock approximation. This supports the (approximate) validity of approximations (3.14)-(3.15). However, it is not known whether eq. (7.2) would be still fulfilled when going farther in the hole line expansion.

Similarly, eq. (2.12) is automatically fulfilled in the $M_1 + M_2$ approximation as we indicated. Using (2.3), (2.13), (2.14), (3.6), (3.7), and eq. (7.3) of ref. [1]), one can easily verify that the sum rule (2.7) is fulfilled in the $M_1 + M_2$ approximation. We point out that in sect. 6 we did not investigate all the E-dependence of S and for that reason, eq. (6.4) is not conserving. Finally, eqs. (2.8), (2.13), (2.14) imply that

$$\text{sgn Im } M(k, E-\mu) = -\text{sgn}\,(E-\mu)\,. \tag{7.3}$$

In table 1, we report on the calculated (on shell) values of Im $(M_1 + M_2)$ at the approximate chemical potential $\tilde{\mu}$: they turn out to be small compared to the typical values of Im $M(k, E)$.

In table 1, we indicate also the values of the internal energy per particle in the $M_1 + M_2$ approximation with self-consistency (3.10) and compare them with the M_1 approximation with self-consistency (3.9). We see that this quantity is lowered when

TABLE 1

Numerical values of the approximate chemical potential $\tilde{\mu}$ (eq. (3.14)), of the free energy per nucleon F/A, of the internal energy per nucleon U/A and of the imaginary part of the mass operator for three temperatures T.

	T	0	7	10
M_1+M_2 approximation	$\tilde{\mu}$	−21.12	−26.10	−26.80
	F/A	−16.55	−20.90	−24.57
	U/A	−16.55	−15.07	−13.54
	Im M	0	−1.0	−2.0
M_1 approximation	$\tilde{\mu}$	−26.12	−28.38	−29.38
	F/A	−13.50	−16.68	−20.29
	U/A	−13.50	−12.0	−11.0

The upper part refers to the $M_1 + M_2$ approximation with self-consistency (3.10). The lower part corresponds to the M_1 approximation with self-consistency (3.9). All quantities are in MeV.

going to the $M_1 + M_2$ approximation. At this degree of approximation, the saturation properties are probably worsened. Here, we did not try to improve upon this point. According to some authors, this can be done by several methods [50,51,16,24]) whose implication and discussion go beyond the scope of this paper.

8. Conclusion

We have concentrated our attention on single-particle properties of nuclear matter both at zero and finite temperature. We have calculated, within the frame of a Brueckner approach, the average field, up to second order in the renormalized interaction. This had never been done before with a fully realistic interaction. [In ref. [52]), a microscopic calculation is performed with the same interaction, however limited to first order.] Compared to the usual Brueckner-Hartree-Fock approximation, the so-called correlation contribution itself is introduced to the mean field. The latter accounts for the influence of possible correlations (of the 2p-2h type) present in the ground state on the propagation of a particle added to the system and for the influence of possible creation of 2h-1p excitations on the propagation of a hole. This addition of the correlation contribution is certainly better from the physical point of view. Essentially, it is quantitatively important for single-particle states below k_F. We obtain an improvement of the predictions for the real part of the average field, if one identifies this quantity in nuclear matter with the one felt by the nucleons in deep-lying states in nuclei.

In our calculation, the average field can be decomposed into a M_1 contribution, which describes the polarization of the medium and a M_2 contribution, which comes from the correlations. This physical picture applies to particle states. Our results show that both contributions to the mean field decrease in absolute value when the temperature increases, but the temperature dependence is stronger for the polarization contribution.

One of our main motivations was the study of the nucleon effective mass m^* and especially its temperature dependence. We confirm that at $T = 0$, m^* exhibits a peak around k_F. We also found that the peak gradually decreases when the matter is heated up. The most important results however are the following: (i) the peak decreases slowly compared to the situation where the correlation graph is neglected; (ii) the value of m^* below k_F is ~ 0.8 for all the temperatures up to 10 MeV. So, even at $T = 0$, the situation is different from what it is when the correlation graph is neglected.

We also investigated the effects of the correlations on the momentum distribution at large k, which seems to be exponentially decreasing, and on the spectral function, for which we showed that the energy dependence of the imaginary part of the correlation graph is important in the description of the spreading of the hole states.

Several problems deserve further attention. The first one is the problem of the self-consistency requirement. We have included the correlation graph itself in the

self-consistent determination of the single-particle energies entering in the calculation of the g-matrix. There is no compelling argument for doing so. One interest of our choice is that it provides a (quasi)-conserving approximation, as we explained in sect. 7. Moreover, if the effective mass is to be calculated by relation (4.1), it is better to use the same choice in the perturbative calculation of the mass operator. For a potential like the Paris potential, the perturbative series of M is unfortunately not converging very fast with this choice. On the other hand, it seems that the same choice (3.10) deteriorates the apparent converging properties for the binding energy [53]) and for the momentum distribution (compared to the more conventional choice (3.9)). For the latter two quantities, the usual choice (3.9) appears to be more efficient. In particular, self-consistency (3.10) does not guarantee all the usual cancellations between graphs containing bubble insertions and those with potential insertions [1,11]), in the expansion of the energy. The same seems to hold for the expansion of $\rho(k)$. This raises an important question of knowing whether the self-consistency should be chosen differently depending upon the quantity under investigation. This is an important problem which goes however beyond the scope of this paper.

Other problems are linked with the physical interpretation of our results. For instance, we still do not know whether the correlation contribution is very much dependent on the fundamental interaction or whether it is dominated by phase space. Also, the relation of our results with non-equilibrium methods, like the Landau–Vlassov equation, should be investigated. For instance, our predictions for the effective mass should influence the general transport properties of nuclear matter. Also, the full energy dependence of the spectral function is certainly worthy of study.

Finally, the density dependence of the correlation graph deserves an extensive study. To our knowledge, this has been investigated in ref. [20]) only, where a linear dependence is quoted.

We are very grateful to the FNRS Belgium, for the opportunity of using a CRAY-XMP computer. Two of us (A.L. and J.C.) would like to thank the CRN Strasbourg for the kind hospitality extended to them. We are also very grateful to Prof. C. Mahaux for helpful discussions and for bringing to our knowledge the results of ref. [37]).

Appendix A

EXPLICIT FORMULAE FOR THE CORRELATION CONTRIBUTION

The correlation contribution to the mass operator (3.7) is, with the notation of sect. 2:

$$M_2(k,E)=\tfrac{1}{2}\sum_{jla} n(j)n(l)(1-n(a))\frac{|\langle ka|g[e(j)+e(l)]|\widetilde{jl}\rangle|^2}{E+e(a)-e(j)-e(l)-i\varepsilon}. \qquad \text{(A.1)}$$

Let

$$\boldsymbol{q}' = \tfrac{1}{2}(\boldsymbol{j} - \boldsymbol{l}), \qquad \boldsymbol{q} = \tfrac{1}{2}(\boldsymbol{k} - \boldsymbol{a}), \qquad \boldsymbol{Q} = \tfrac{1}{2}(\boldsymbol{k} + \boldsymbol{a}). \tag{A.2}$$

Using a partial wave decomposition of the g-matrix [18]) and the usual angle-averaging procedure [18,54]), one obtains:

$$M_2(k, E) = \frac{8}{\pi^2 k} \iint \mathrm{d}q\, \mathrm{d}Q\, qQ[1 - n(\sqrt{2q^2 + 2Q^2 - k^2})] \int \mathrm{d}q'\, q'^2 P(q', Q)$$

$$\times \sum_{JTSLL'} (2J+1)(2T+1) \frac{|g^{JTS}_{LL'}(q, q', Q; e_+ + e_-)|^2}{E + e(\sqrt{2q^2 + 2Q^2 - k^2}) - e_+ - e_- - i\varepsilon}, \tag{A.3}$$

where

$$e_\pm = e([q'^2 + Q^2 \pm 2\sqrt{\tfrac{1}{3}} q' Q P(q', Q)]^{1/2}). \tag{A.4}$$

We have still to specify the domain of variation for the variables q, Q and q'. For finite temperature there is no restriction and the quantity $P(q', Q)$, which represents the angle-averaged value of $n(\boldsymbol{j})n(\boldsymbol{l})$, is given by, in the approximation $e(k) = e_0 + bk^2$ (see ref. [3])):

$$P(q', Q) = \frac{1}{1 - \exp(2A)} \left\{ 1 + \frac{1}{B} \ln \frac{1 + \exp(A - B)}{1 + \exp(A + B)} \right\}, \tag{A.5}$$

with

$$A = \beta(e_0 - \mu) + \beta b(q'^2 + Q^2), \qquad B = 2\beta b q' Q, \tag{A.6}$$

and, of course $\beta \equiv T^{-1}$.

For $T = 0$, it is more economical to delineate exactly the domain of variation of the variables. This may be helpful also for numerical integration at $T \neq 0$. The variable q' is restricted to

$$q' \leq k_\mathrm{F}. \tag{A.7}$$

The quantities q and Q are limited to

$$\tfrac{1}{2}(k_\mathrm{F} - k) \leq q \leq \tfrac{1}{2}(k_\mathrm{F} + k), \qquad \sqrt{\tfrac{1}{2}(k^2 + k_\mathrm{F}^2) - q^2} \leq Q \leq q + k \tag{A.8a}$$

or

$$q \geq \tfrac{1}{2}(k + k_\mathrm{F}), \qquad |q - k| \leq Q \leq q + k \tag{A.8b}$$

when $k < k_\mathrm{F}$, and to

$$\tfrac{1}{2}(k - k_\mathrm{F}) \leq q \leq \tfrac{1}{2}(k_\mathrm{F} + k), \qquad \sqrt{\tfrac{1}{2}(k^2 + k_\mathrm{F}^2) - q^2} \leq Q \leq q + k, \tag{A.9a}$$

or

$$0 \leq q \leq \tfrac{1}{2}(k - k_\mathrm{F}), \qquad |q - k| \leq Q \leq q + k, \tag{A.9b}$$

or

$$q \geq \tfrac{1}{2}(k+k_F), \qquad |q-k| \leq Q \leq q+k, \tag{A.9c}$$

when $k > k_F$. The function $P(q', Q)$ is then given by

$$P(q', Q) = \begin{cases} 1, & \text{for } 0 \leq q' \leq k_F - Q, \\ \dfrac{k_F^2 - q'^2 - Q^2}{2q'Q}, & \text{for } k_F - Q \leq q' \leq \sqrt{k_F^2 - Q^2}, \\ 0, & \text{for } \sqrt{k_F^2 - Q^2} \leq q' \leq k_F \text{ or for } Q > k_F. \end{cases} \tag{A.10}$$

We took advantage of the fact that the g-matrix is known to weakly depend upon the total c.m. momentum Q and evaluate it only at the average value Q_{av}, which we define as

$$Q_{av}^2 = \frac{\int d^3Q\, Q^2 n(|q'+Q|) n(|q'-Q|)}{\int d^3Q\, n(|q'+Q|) n(|q'-Q|)}. \tag{A.11}$$

Taking also Q_{av} in the energy denominator in eq. (A.3), the remaining integral over Q is performed once for all.

We first calculate the g-matrix $g_{LL'}^{JTS}$ over a set of mesh points in (q, q') for each partial wave up to ${}^1H_5$. An extension of the matrix inversion technique of ref. [55]) is used, which takes proper account of the singularities of the energy denominator introduced by the continuous single-particle spectrum. Performing the partial wave summation, we obtain a function $\mathcal{G}(q, q')$ which can be interpolated when necessary. For a given E, we then search for poles of the denominator in eq. (A.3) and treat the principal part integral over q' as in ref. [3]). The imaginary part of $M_2(k, E)$ is obtained straightforwardly once the poles have been determined. For model interactions of the type used in ref. [23]), we checked that at $T = 0$, this procedure fully agrees with the approach based on dispersion relations. Let us finally notice that we calculate $\rho(k)$ by evaluating $M_1(k, E)$ and $M_2(k, E)$ at the two values $E = e(k) \pm \Delta$ with $\Delta = 4$ MeV.

References

1) J.-P. Jeukenne, A. Lejeune and C. Mahaux, Phys. Reports **25C** (1976) 83
2) R. Malfliet and B. ter Haar, Phys. Reports, to be published
3) A. Lejeune, P. Grangé, M. Martzolff and J. Cugnon, Nucl. Phys. **A453** (1986) 189
4) A.L. Fetter and J.D. Walecka, Quantum theory of many-particle systems (McGraw-Hill, N.Y., 1971)
5) A.A. Abrikosov, L.P. Gorkov and I.E. Dzyaloshinski, Methods of quantum field theory in statistical physics (Prentice Hall, N.Y., 1963)
6) P. Nozières, Theory of interacting fermi systems (Benjamin, N.Y., 1964)
7) L.P. Kadanoff and G. Baym, Quantum statistical mechanics (Benjamin, N.Y., 1962)
8) E.M. Lifshitz and L.P. Pitaevskii, Statistical physics (Pergamon, N.Y., 1980)
9) T. Matsubara, Prog. Theor. Phys. **14** (1955) 351

10) S.D. Yang and T.T.S. Kuo, preprint, 1986
11) B.D. Day, Rev. Mod. Phys. **50** (1978) 495
12) A.D. Jackson, Ann. Rev. Nucl. Part. Sc. **33** (1983) 105
13) R. Sartor, Nucl. Phys. **A289** (1977) 329
14) A. Lejeune and C. Mahaux, Nucl. Phys. **A295** (1978) 189
15) M. Lacombe, B. Loiseaux, J.M. Richard, R. Vinh Mau, J. Côté, D. Pirès and R. de Tourreil, Phys. Rev. **C21** (1980) 861
16) C.A. Engelbrecht and H.A. Weidenmüller, Nucl. Phys. **A184** (1972) 385
17) P.E. Hodgson, Rep. Prog. Phys. **47** (1984) 613
18) K.A. Brueckner and J.L. Gammel, Phys. Rev. **109** (1958) 1023
19) K.A. Brueckner, J.L. Gammel and J.T. Kubis, Phys. Rev. **118** (1960) 1438
20) H.S. Köhler, Phys. Rev. **137** (1965) B1145
21) R. Sartor, Nucl. Phys. **A267** (1976) 29
22) R. Sartor and C. Mahaux, Phys. Rev. **C21** (1980) 1546
23) V. Bernard and C. Mahaux, Phys. Rev. **C23** (1981) 888
24) H. Orland and R. Schaeffer, Nucl. Phys. **A299** (1978) 442
25) R.W. Hasse and P. Schuck, Nucl. Phys. **A445** (1985) 205
26) G.E. Brown, J.H. Gunn and P. Gould, Nucl. Phys. **46** (1963) 598
27) W. Brenig, Z. Phys. **202** (1967) 58
28) G.F. Bertsch and T.T.S. Kuo, Nucl. Phys. **A112** (1968) 204
29) V. Bernard and Nguyen Van Giai, Nucl. Phys. **A348** (1980) 75
30) G.F. Bertsch, P.F. Bortignon and R.A. Broglia, Rev. Mod. Phys. **55** (1983) 287
31) J. Cugnon, P. Grangé and A. Lejeune, Phys. Rev. **C35** (1987) 86
32) C. Gale, G. Bertsch and S. Das Gupta, UMSI preprint, Nov. 1986
33) A.B. Migdal, Nucl. Phys. **30** (1962) 239
34) C. Mahaux and H. Ngô, Phys. Lett. **100B** (1981) 285
35) S. Fantoni and V.R. Pandharipande, Nucl. Phys. **A427** (1984) 473
36) J.P. Blaizot and B.L. Friman, Nucl. Phys. **A372** (1981) 69
37) C. Mahaux and R. Sartor, Phys. Rev. Lett. **57** (1986) 3015, and private communication
38) H.A. Bethe, Ann. Rev. Nucl. Sci. **21** (1971) 93
39) G. Nebbia *et al.*, Phys. Lett. **B176** (1986) 20
40) N. Vinh Mau and D. Vautherin, Nucl. Phys. **A445** (1985) 245
41) R. W. Hasse and P. Schuck, Phys. Lett. **B179** (1986) 313
42) C. Mahaux, R. Broglia, P.F. Bortignon and C. Dasso, Phys. Reports **120** (1985) 1
43) D.J. Thouless, The quantum mechanics of many-body systems, 2nd ed. (Academic Press, N.Y., 1972)
44) A.B. Migdal, JETP (Sov. Phys.) **5** (1957) 333
45) H. Krivine, Nucl. Phys. **A457** (1986) 125
46) M. Jaminon, C. Mahaux and H. Ngô, Nucl. Phys. **A452** (1986) 445
47) V.R. Pandharipande, C.N. Papanicolas and J. Wambach, Phys. Rev. Lett. **53** (1984) 1133
48) B.D. Day, unpublished
49) N.M. Hugenholtz and L. Van Hove, Physica **24** (1958) 363
50) D.S. Koltun, Phys. Rev. **C9** (1974) 484
51) K. Davies and R. McCarthy, Phys. Rev. **C4** (1971) 81
52) L. Rikus, N. Nakano and N. H. von Geramb, Nucl. Phys. **A414** (1984) 413
53) P. Grangé and A. Lejeune, Nucl. Phys. **A327** (1979) 335
54) D.W.L. Sprung, Advances in Nuclear Physics, vol. 5, ed. by M. Baranger and E. Vogt (Plenum, N.Y., 1972)
55) M.I. Haftel and F. Tabakin, Nucl. Phys. **A158** (1970) 1